The Rate Enhancement Produced by the Ribosome: An Improved Model†

Gottfried K. Schroeder and Richard Wolfenden*

Department of Biochemistry and Biophysics, University of North Carolina, Chapel Hill, North Carolina 27599

Received December 19, 2006; Revised Manuscript Received January 31, 2007

ABSTRACT: As a model for mechanistic comparison with peptidyl transfer within the ribosome, the reaction of aqueous glycinamide with *N*-formylphenylalanine trifluoroethyl ester (fPhe-TFE) represents an improvement over earlier model reactions involving Tris. The acidity of trifluoroethanol (pK_a 12.4) resembles that of tRNA (12.98) more closely than do the acidities of model reactants described earlier, and the reactivity of the simple nucleophile glycinamide is free of potential complications that arise from alternative reaction pathways available to Tris. At 25 °C, the uncatalyzed reaction of glycinamide with fPhe-TFE proceeds with a second-order rate constant of 3×10^{-5} M^{-1} s^{-1}; $\Delta H^{\ddagger} = +7.8$ kcal/mol; $T\Delta S^{\ddagger} = -15.7$ kcal/mol. The ribosomal reaction of puromycin with fMet-tRNA proceeds 3×10^7-fold more rapidly, with a second-order rate constant (k_{cat}/K_m) of 1×10^3 M^{-1} s^{-1}; $\Delta H^{\ddagger} = +16.0$ kcal/mol; $T\Delta S^{\ddagger} = +2.0$ kcal/mol. That rate enhancement, an order of magnitude larger than estimated earlier, is fully explained by the more favorable entropy of activation of the ribosomal reaction. Experiments involving ethylene glycol esters suggest that neighboring −OH group effects are negligible in the presence of solvent water, which itself acts as a general base catalyst. In the desolvated interior of the ribosome, the vicinal 2′-OH group of aminoacyl-tRNA probably replaces water as a general base catalyst. But the catalytic effect of the ribosome itself is overwhelmingly entropic in origin, suggesting that the ribosome achieves its effect by physical desolvation and/or juxtaposition of the reactants in a manner conducive to peptidyl transfer.

In enzyme-catalyzed reactions that involve a single substrate and hydrolytic reactions in which the second substrate (water) cannot be elevated much above its concentration in cellular fluid, enzymes have been found to produce a major reduction in the enthalpy of activation ($\Delta H^{\ddagger}$). Those enzymes produce relatively minor changes in the entropy of activation ($T\Delta S^{\ddagger}$), with an average effect near zero (*1*). In two-substrate reactions, which are common in biosynthesis, an enzyme must often gather two substrates from dilute solution and bind them noncovalently in a configuration that is conducive to reaction. In itself, this "gathering" effect might in principle produce a very large rate enhancement (*2*). After two substrates have been bound, the enzyme's active site may also participate in the reaction as a chemical catalyst, using additional forces of attraction to stabilize chemical intermediates that approach the transition state in structure. In such a two-substrate reaction, the dissociation constant of the enzyme's complex with the combined substrates in the transition state is expected to be lower than the product of the dissociation constants of each of the two substrates by a factor that matches or exceeds the factor by which the turnover number (k_{cat}) of the EAB complex exceeds the second-order rate constant of the uncatalyzed reaction under otherwise similar conditions (*3*).

How substantial a role does entropy reduction play in the catalytic effects of two-substrate enzymes, and is there a significant disparity between their behavior and the behavior of enzymes catalyzing simpler reactions? The possibility that entropy might play a substantial role in enzyme catalysis of multisubstrate reactions can be tested by determining the rate of a two-substrate reaction in the absence of a catalyst, and of the corresponding reaction in the presence of an enzyme, as a function of changing temperature. One interesting case in which that question has arisen is the peptidyl-transferase center of the ribosome. According to Crick's original "adapter" hypothesis (*4*), the ribosome and mRNA might be expected to act partly (or perhaps entirely) as a "marriage broker" that brings one molecule of peptidyl-tRNA together with one molecule of aminoacyl-tRNA. To what extent do proximity effects account for the activity of the ribosome, and to what extent does the peptidyl-transferase center of the ribosome "recognize" distinctive chemical features of the altered substrates in the transition state (such as electrostatic charge and optimal geometry), and so act as a catalyst in a more "chemical" sense? A strong entropic component would favor the first answer, and a strong enthalpic component would favor the second.

Answers to these questions would be helpful in understanding the action of multisubstrate enzymes. They might also be of practical value in indicating whether, in designing inhibitors of such enzymes, it would be sufficient simply to combine the binding determinants of the two substrates. A striking example of a potential bisubstrate analogue inhibitor is CCdApPuromycin, designed by Yarus et al. to resemble peptidyl-tRNA and aminoacyl-tRNA at the moment of their reaction to form a new peptide bond (*5*). Indeed, the peptidyl-transferase center of the ribosome, composed entirely of RNA, was first identified by locating the site of binding of

† This work was supported by National Institutes of Health Grant GM-18325.

* To whom correspondence should be addressed. Phone: (919) 966-1203. Fax: (919) 966-2852. E-mail: water@med.unc.edu.

10.1021/bi602600p CCC: $37.00
Published on Web 03/13/2007

Table 1: pK_a Values of Model Reactant Groups and Their *Ribosomal* Counterparts

acyl group transferred	pK_a	attacking amine	pK_a	leaving group alcohol	pK_a
N-formylphenyl-alanine	3.3[a]	glycinamide	8.2[b]	2,2,2,-trifluoro-ethanol	12.4[c]
peptidyl-tRNA	*3.4*[d]	*aminoacyl-tRNA′*	*8.1*[e]	*tRNA*	*12.98*[f]

[a] Supporting Information, Text 1 and Reference *21*. [b] Reference *22*. [c] Reference *23*. [d] Reference *24*. [e] Reference *14*. [f] Reference *19*.

the Yarus inhibitor (*6*). The effectiveness of this inhibitor is consistent with the view that the amino group of aminoacyl-tRNA (bound at the A site) attacks the ester linkage between the carboxylate group of the growing peptide chain and the 3′-OH group (*7*) of peptidyl-tRNA (bound at the P site). Recent biochemical and mutagenesis studies suggest that the ribosome is unlikely to act as an acid/base catalyst (*8*−*12*), but many aspects of the mechanism of peptide bond formation within the ribosome are still under debate.

Earlier, reactions of methyl and ethylene glycol esters of *N*-formylglycine (fGly-OMe and fGly-glycol, respectively) with the primary amino group of tris(hydroxymethyl)-aminomethane (Tris) were examined as possible models for peptidyl transfer in the ribosome.[1] Comparing the second-order rate constants for these model reactions in water with the second-order rate constant observed for peptidyl transfer within the ribosome, the ribosome was found to enhance the rate of reaction by a factor of $\sim 3 \times 10^6$ at 25 °C (*13*, *14*). That rate enhancement was found to be entirely entropic in origin, the heat of activation for the model reaction in water being considerably more favorable than the heat of activation for peptidyl transfer within the ribosome. That observation seemed consistent with two possibilities. It was suggested that the purely entropic advantage of the ribosome might arise from its ability to juxtapose the reactants in a position conducive to reaction, or from its ability to avoid the entropic cost of organizing solvent water around the (presumably zwitterionic, *15*) transition state for peptidyl transfer.

The reactants chosen for examination in the model reactions described above were deficient, however, in certain respects. First, any of the three −OH groups of Tris might serve as an initial site of acylation (in a reaction that might be subject to intramolecular catalysis by the primary amino group of Tris) followed by O-to-N migration. Such behavior has been observed in some aminolysis reactions of Tris (*16*, *17*), although not in others (*18*). If O-to-N migration did indeed occur, Tris might be correspondingly *more* reactive than other primary amines for which that ambiguity does not exist, including aminoacyl-tRNA. Second, the basicity of the conjugate base of trifluoroethanol (pK_a = 12.4, see Table 1) more closely approximates the basicity of the leaving 3′-OH group of the terminal adenosine of tRNA (pK_a = 12.98, *19*) than do those of ethylene glycol (pK_a = 14.8, *20*) or methanol (pK_a = 15.5, *20*), which were used in the previous study. The inherent reactivity of esters containing these model leaving groups might then be *less* than the inherent reactivity of esters of tRNA. The effects of these potential shortcomings on reactivity would be expected to oppose each other to some unknown extent. Finally, in contrast with the reaction of phenyl acetate with methylamine (*15*), general base catalysis by a second molecule of amine was not observed for the reaction of Tris with these esters. The absence of general base catalysis suggests that the behavior of Tris might be atypical in some respects, rendering its reactions inappropriate for comparison with the aminolysis of peptidyl-tRNA.

To circumvent those difficulties, it seemed desirable to examine the behavior of model reactants bearing a closer resemblance to the biological reactants. In the present work, we examined the reaction of fPhe-TFE with glycinamide, whose free amino group serves unambiguously as the nucleophile in acyl transfer (Scheme 1 and Table 1). The thermodynamics of activation were also determined for the uncatalyzed reaction, to allow comparison with those of the reaction in the ribosome (*13*, *14*). Several related reactions were also characterized, to establish the effects of varying structure on reactivity.

MATERIALS AND METHODS

N-Formylalanine methyl ester (fAla-OMe) and *N*-formylphenylalanine methyl ester (fPhe-OMe) were purchased from BACHEM Biosciences Inc. (King of Prussia, PA). 2,2,2-Trifluoroethyl formate was purchased from SynQuest Laboratories Inc. (Alachua, FL). Other compounds, unless otherwise noted or described below, were purchased from Sigma-Aldrich, Inc.

N-Formylphenylalanine Trifluoroethyl Ester (fPhe-TFE). *N*-Formylphenylalanine (TCI America; 3.6 mmol) was treated with HCl-saturated 2,2,2-trifluoroethanol (10 mL) for ∼3.5 days at room temperature. After removal of the solvent by evaporation, the product was dissolved in 50% aqueous methanol containing sodium acetate (0.1 M) and purified by reverse-phase HPLC (Whatman Partisil 10 ODS-2, 22 × 500 mm) using a linear gradient from 50% methanol to 100% methanol in 1 h at a flow rate of 3 mL/min. The product was eluted after 30 min (∼50% yield), and its identity was confirmed by NMR (Supporting Information, Figure 1) and mass spectrometry (Supporting Information, Figure 2). The only other peaks in the HPLC chromatogram (Supporting Information, Figure 3) corresponded to unreacted starting materials and fPhe-OMe formed by methanolysis during workup. Fractions containing the product were evaporated to dryness and stored under vacuum.

N-Formylphenylalanine Ethylene Glycol Ester (fPhe-glycol). *N*-Formylphenylalanine (TCI America; 0.4 mmol) was treated with dry ethylene glycol saturated with HCl (∼1 mL) for 24 h at room temperature. The starting material was completely consumed, and after removal of the solvent (and byproduct formyl ethylene glycol) by evaporation, the identity of the desired product (∼30% yield, syrup) was confirmed by NMR and mass spectrometry. The only other product of this reaction was the deformylated ethylene glycol ester (∼70% yield). Because the present aminolysis reactions were carried out under pseudo-first-order conditions, and monitored by the resonances arising from formyl protons, the presence of the phenylalanine ethylene glycol ester did not interfere with the analyses described below.

[1] Tris, tris(hydroxymethyl)aminomethane. Amino acid derivatives are abbreviated according to the following conventions (example phenylalanine): fPhe-TFE, *N*-formylphenylalanine trifluoroethyl ester; fPhe-OMe, *N*-formylphenylalanine methyl ester; fPhe-glycol, *N*-formylphenylalanine ethylene glycol ester.

Scheme 1: Chemistry of Peptide Bond Formation[a]

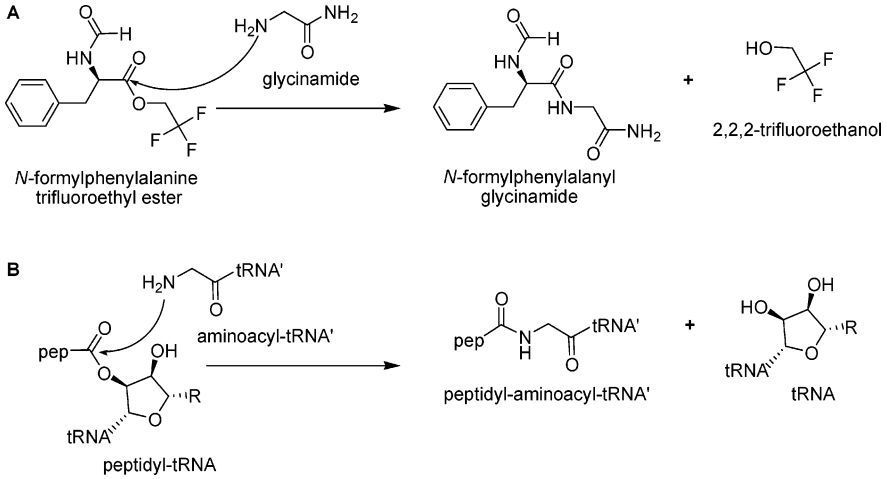

[a] (A) Model reaction between glycinamide and *N*-formylphenylalanine trifluoroethyl ester in aqueous solution. (B) Reaction in the peptidyl-transferase center of the ribosome. Amino-acylated tRNA (aminoacyl-tRNA′, bound in the A-site) attacks the ester linkage of the nascent peptide chain (peptidyl-tRNA, bound in the P-site).

N-Formylalanine Trifluoroethyl Ester (fAla-TFE). *N*-Formylalanine (TCI America; 0.4 mmol) was treated with HCl-saturated 2,2,2-trifluoroethanol (4 mL) for ~1 week at room temperature. After removal of the solvent by evaporation, the identity of the product (~60% yield, ~40% unreacted *N*-formylalanine) was confirmed by NMR and mass spectrometry.

Kinetic Measurements. The present kinetic studies were conducted in 99% D_2O, but since only a slight reduction (~10%) in the rate of the uncatalyzed reaction of phenyl acetate with methylamine was observed in D_2O (*15*), kinetic isotope effects on ester aminolysis rates are expected to be small. Reactions of fPhe-TFE with glycinamide were followed by proton NMR (Varian Inova 600 MHz; Palo Alto, CA), as a function of changing temperature. The temperature of the NMR probe was calibrated with ethylene glycol, using calibration software provided by Varian (VnmrJ, version 1.1c). A buffer solution (1 mL) containing glycinamide (0.4 M), potassium hydroxide (0.2 M), and pyrazine (10^{-3} M, added as an integration standard) in 99% D_2O was preincubated at the final probe temperature. Immediately before data collection, fPhe-TFE (0.5 mg) was quickly dissolved in this solution to produce a final concentration of 10^{-3} M and the progress of reaction was followed by measuring the NMR spectrum at intervals. In these experiments, unprotonated glycinamide was present in large excess (0.2 M) and the decomposition of starting material followed first-order kinetics to completion (Supporting Information, Figure 4). Data were routinely acquired over a period of at least two half-times. A standard water suppression pulse sequence was used with a delay corresponding to 5 times T_1. The value of T_1 was approximated at each temperature using an inversion recovery sequence where $T_1 \approx t_{null}/\ln(2)$. The calculated value of T_1 at 18 °C (10.7 s) was also used for the experiments at 11 °C and 4 °C. At least 20 data points were collected at each temperature, using a minimum of 8 transients for each point. The integrated intensities of the formyl proton peaks of the starting material, the aminolysis product, and the hydrolysis side product, estimated with reference to the internal pyrazine standard, were then fit to the appropriate rate equations by nonlinear regression, using SigmaPlot (Systat Software, Point Richmond, CA), as described in Results.

Effects of Ionic Strength, Buffer Concentration, and pH. All reactions were conducted at 25 °C in D_2O and followed by 600 MHz ^1H NMR. The pulse sequence was similar to that used in the temperature dependence experiments, but used only 4 transients. Increasing amounts of KCl were added to a solution containing a fixed concentration of unprotonated glycinamide (0.1 M) and ester (10^{-3} M). The effect of changing glycinamide concentration was tested by allowing fPhe-TFE (1.5×10^{-3} M) to react with increasing amounts of glycinamide in D_2O. The concentration of unprotonated glycinamide was adjusted by adding different amounts of a buffer containing glycinamide (2 M) and potassium hydroxide (1 M). In both sets of experiments, the observed pH value remained constant over the full range of buffer/KCl concentrations. To test the dependence of the reaction on changing pH, a solution of unprotonated glycinamide (0.125 M) was adjusted with either 3 M KOH or 3 M HCl to the appropriate pH value, maintaining the ionic strength at 0.5 M by appropriate addition of KCl, and allowed to react with the model ester (1.5×10^{-3} M). The pD values of the reaction mixtures were estimated by adding 0.408 (*25*) to the observed pH value, measured before and after reaction with fPhe-TFE. Concentrations of ^-OD were calculated using a pK_w value of 14.87 (based on molarity) for D_2O at 25 °C (*26*). Proton NMR data were integrated with reference to pyrazine as an internal standard, as described above. In every case, decomposition of the starting material followed first-order kinetics. The observed first-order rate constant was then divided into its components according to the observed fraction of the overall decomposition of the ester that proceeded by aminolysis and hydrolysis, respectively.

RESULTS

Glycinamide Attack on N-Formylphenylalanine Trifluoroethyl Ester (fPhe-TFE). The reaction of fPhe-TFE with glycinamide was accompanied by hydrolysis, but the rates of aminolysis exceeded those of hydrolysis at all temperatures used in this study. The NMR signals of the starting material and the two products were sufficiently resolved for accurate

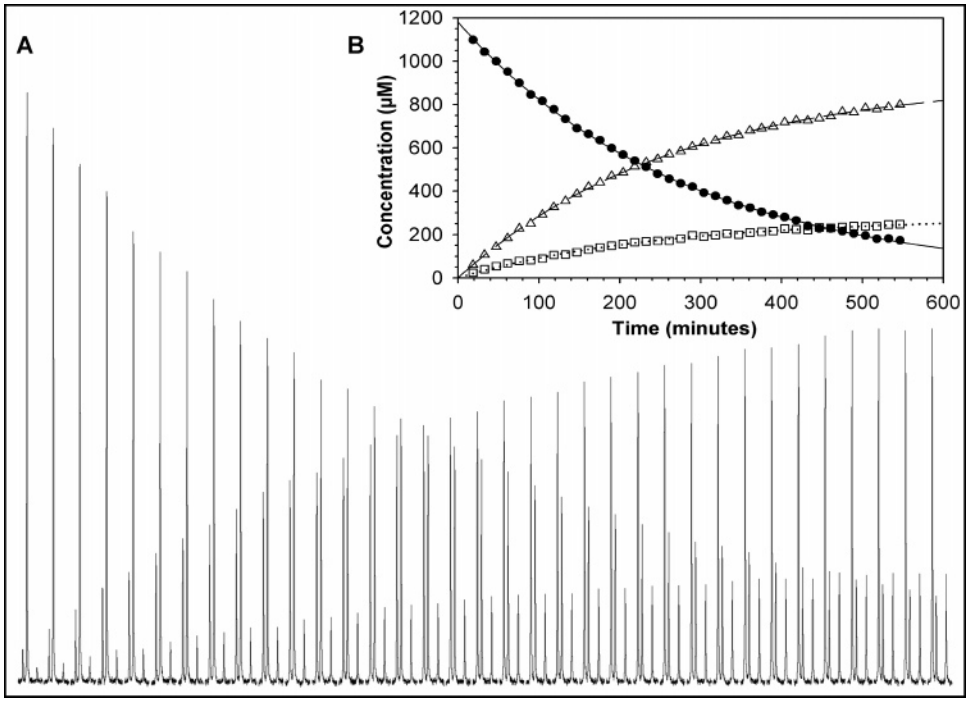

FIGURE 1: Reaction of *N*-formylphenylalanine trifluoroethyl ester and glycinamide at 4 °C monitored by 600 MHz ^{1}H NMR. (A) Real time kinetic data following the formyl protons of the aminolysis product, starting material and hydrolysis product (left to right, respectively) in the range of 8.04 to 7.88 ppm. (B) Integrated data plotted as a function of time for *N*-formylphenylalanyl glycinamide (△), *N*-formylphenylalanine trifluoroethyl ester (●), and *N*-formylphenylalanine (□). Nonlinear regression fit the data satisfactorily ($R^2 > 0.99$): the first curve (solid line) corresponds to exponential decay (eq 3) while the other curves (dashed and dotted lines) correspond to exponential rise to max (eq 5 and eq 6, respectively).

integration through the temperature range between 4 °C and 25 °C. At temperatures above 25 °C, overlap between the product peaks became a significant source of error, so that data acquired above 25 °C could not be used with confidence. A typical set of observations is shown in Figure 1A. In these experiments, we analyzed the full time course of formation of each of the two products using the equations below (see Supporting Information, Text 2):

$$A_1 \xrightarrow{k^{app}_{RNH2}} A_2 \qquad \text{(eq 1)}$$

$$A_1 \xrightarrow{k^{app}_{OH^-}} A_3 \qquad \text{(eq 2)}$$

$$[A_1] = [A_1]_0 e^{-k_T t} \qquad \text{(eq 3)}$$

$$k_T = k^{app}_{RNH2} + k^{app}_{OH^-} \qquad \text{(eq 4)}$$

$$[A_2] = \frac{k^{app}_{RNH2}[A_1]_0}{k_T}[1 - e^{-k_T t}] \qquad \text{(eq 5)}$$

$$[A_3] = \frac{k^{app}_{OH^-}[A_1]_0}{k_T}[1 - e^{-k_T t}] \qquad \text{(eq 6)}$$

$$k^{app}_{RNH2} = k_{RNH2}[RNH_2] \qquad \text{(eq 7)}$$

where A_1 = *N*-formylphenylalanine trifluoroethyl ester, A_2 = *N*-formylphenylalanyl glycinamide, A_3 = *N*-formylphenylalanine, t = time, and RNH_2 = glycinamide. Correlation of the integrated data (Figure 1B) obtained at different time points was satisfactory ($R^2 > 0.99$). The aminolysis product

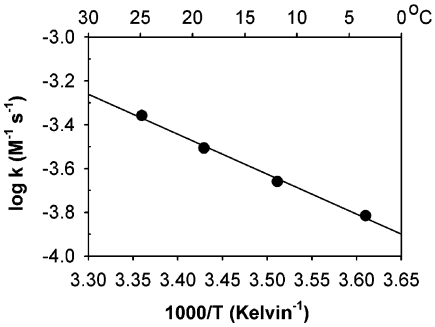

FIGURE 2: Arrhenius plot of the second-order rate constants for the aminolysis of fPhe-TFE by glycinamide. The concentration of unprotonated amine used for the calculation of the second-order rates was based on the temperature dependence of the dissociation constant of glycinamide in D_2O.

of the reaction was also isolated using HPLC and unequivocally identified using mass spectrometric analysis (Supporting Information, Figure 5). The formyl proton resonance (8.01 ppm) of the isolated material was identical with that of the peak (△) indicated in Figure 1. The second-order rate constants (k_{RNH2}) observed at each temperature are shown as an Arrhenius plot in Figure 2. Each value was corrected for the shift in the concentration of unprotonated glycinamide as a function of temperature, according to the experimentally determined constant $\Delta pK_a/°C = -0.025$ (Supporting Information, Figure 6). Linear regression analysis (Figure 2) yielded an activation energy, E_a, of 8.4 kcal/mol. The hint of curvature in Figure 2 suggests a slight difference in heat capacity between the substrates in the ground state and the transition state, but minor uncertainties in the concentration of amine in the free base form might be responsible for this apparent departure from linearity. The activation enthalpy

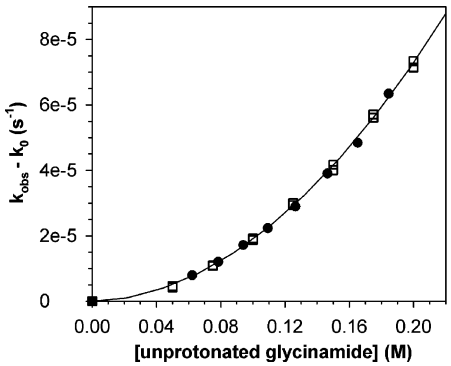

FIGURE 3: Plot of the apparent fPhe-TFE aminolysis rate constant (where k_{obs} = observed rate constant and k_0 = apparent hydrolysis rate constant) versus the concentration of unprotonated glycinamide. The concentration of glycinamide in the free base form was adjusted either by the addition of glycinamide while maintaining a constant pD (□) or by varying the pD at a fixed concentration of glycinamide (●). The curve shown corresponds to a 2-parameter quadratic (see eq 8).

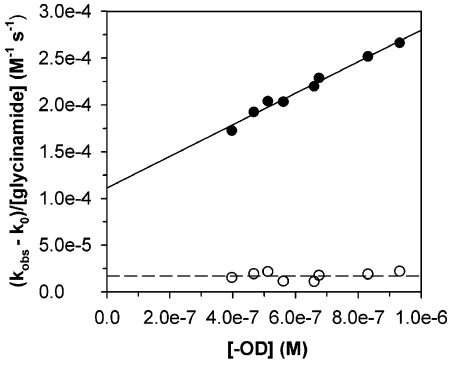

FIGURE 4: Plot of the apparent second-order fPhe-TFE aminolysis rate constant (where k_{obs} = observed rate constant and k_0 = apparent hydrolysis rate constant) versus the concentration of $^-$OD. The solid line represents a linear fit to the observed aminolysis rate data (●) while the dashed line is a straight line that corresponds to the average value for the aminolysis rate when adjusted for the contribution of amine catalysis (○).

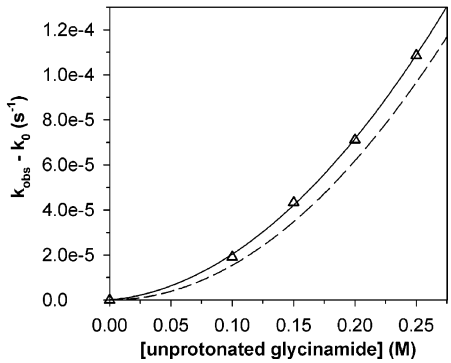

FIGURE 5: Plot of the apparent fAla-TFE aminolysis rate constant (where k_{obs} = observed rate constant and k_0 = apparent hydrolysis rate constant) versus the concentration of unprotonated glycinamide. The lower curve (dashed line) corresponds to a 1-parameter quadratic fit and represents the contribution of amine catalysis to the observed aminolysis rate (△). The upper curve (solid line) corresponds to a 2-parameter quadratic fit and includes the uncatalyzed contribution to the observed aminolysis rate.

for the aminolysis reaction ($\Delta H^{\ddagger}$ = 7.8 kcal/mol at 25 °C) was calculated using the relationship $E_a = \Delta H^{\ddagger} - RT$. That value is similar to the value ($\Delta H^{\ddagger}$ = 8.5 kcal/mol) determined by Jencks et al. (*15*) for the uncatalyzed rate of aminolysis of phenyl acetate by methylamine. Because hydroxide attack is more sensitive to temperature than aminolysis, the fraction of k_T represented by hydroxide attack varied from 20% at 4 °C to 40% at 25 °C (for further discussion of the reaction with hydroxide ion see Supporting Information, Text 3).

Effects of Buffer Concentration, pH, and Ionic Strength. Rate constants for aminolysis and hydroxide attack were obtained by apportioning the overall first-order rate constant for substrate decomposition, k_T (eq 4), according to the observed ratio of products (which did not vary during the course of reaction). Figure 3 shows the apparent rate constant for aminolysis, k^{app}_{RNH2}, plotted against the concentration of unprotonated glycinamide. [In accordance with the relationship described in eq 4, the ($k_{obs} - k_0$) term in Figure 3 is equivalent to ($k_T - k^{app}_{OH^-}$); this new convention is adopted throughout the manuscript.] The upward curvature of this plot is consistent with the presence of both an uncatalyzed and an amine-catalyzed term in the rate equation and can be analyzed in terms of eq 8, where k_1 = the uncatalyzed rate and k_2 = the catalytic contribution of the buffer, as observed for the reaction of phenyl acetate with methylamine (*15*). Fitting these data to eq 8 ($R^2 > 0.99$) yielded $k_1 = 3.0 \times 10^{-5}$ M^{-1} s^{-1} for uncatalyzed aminolysis and $k_2 = 1.7 \times 10^{-3}$ M^{-2} s^{-1} for amine-catalyzed aminolysis, at 25 °C.

$$k^{app}_{RNH2} = k_1[RNH_2] + k_2[RNH_2]^2 \qquad \text{(eq 8)}$$

Included in Figure 3 are data obtained under two sets of experimental conditions: (a) varying the concentration of glycinamide at constant pD and (b) varying the concentration of the conjugate base of glycinamide by adjusting the pD, at a fixed concentration of glycinamide. Both sets of data show the same dependence on glycinamide concentration (eq 8). Apparent second-order rate constants for aminolysis, adjusted for the contribution of amine catalysis (k_2) and the change in the concentration of unprotonated amine, were found to be independent of pD over a range of ~0.5 log units centered about the pK_a of glycinamide (Figure 4). The finding that the *observed* aminolysis rate constant increases with increasing pD in proportion to the concentration of free amine, and that the value of k_1 is independent of the [$^-$OD], indicates that aminolysis proceeds exclusively by attack of the conjugate base of glycinamide. Addition of the nonpolar solvent tetrahydrofuran (10% v/v) reduced the observed aminolysis rate by about 35% (Supporting Information, Figure 7). That solvent effect is consistent with a reaction between two neutral species to form a more polar transition state (*15*). For reasons that are unclear, the rate of aminolysis did not vary with ionic strength between 0.25 and 2.75 M KCl (Supporting Information, Figure 8).

The observed free energy of activation for ester aminolysis ($\Delta G^{\ddagger}$) was 23.5 kcal/mol. Using the relationship $\Delta G^{\ddagger} = \Delta H^{\ddagger} - T\Delta S^{\ddagger}$, the activation entropy was estimated to be −15.7 kcal/mol at 25 °C.

Glycinamide Attack on Other Model Esters. A plot of the observed fAla-TFE aminolysis rate as a function of the concentration of unprotonated glycinamide (Figure 5) fit eq 8 satisfactorily ($R^2 > 0.99$, solid line). The resulting values of k_1 and k_2 were similar to those observed for fPhe-TFE (Table 2). The dashed line, representing k_2 for the catalyzed rate alone, matched the data with $R^2 = 0.95$. The difference between the two curves corresponds to k_1, the uncatalyzed

Table 2: Rate Constants for Aminolysis by Glycinamide of Various Model Esters

model ester	catalyzed rate (M^{-2} s^{-1})	uncatalyzed rate (M^{-1} s^{-1})
fPhe-TFE	1.7×10^{-3}	$3 \pm 2 \times 10^{-5}$
fAla-TFE	1.5×10^{-3}	$5 \pm 2 \times 10^{-5}$
formyl-TFE[a]	7.3×10^{-1}	$5 \pm 2 \times 10^{-3}$
fPhe-glycol	1.4×10^{-5}	$1 \pm 0.4 \times 10^{-6}$
fPhe-OMe	6.0×10^{-6}	$4 \pm 1 \times 10^{-7}$
fAla-OMe	6.8×10^{-6}	$1 \pm 0.4 \times 10^{-7}$
fGly-OMe	6.0×10^{-5}	(masked)[b]

[a] TFE formate, a model for fGly-TFE. [b] A single parameter fit was sufficient to account for the observed rate data.

(or water-catalyzed; see Discussion) contribution to the observed rate of aminolysis.

The same procedure was applied to formyl-TFE (trifluoroethyl formate, representing *N*-formylglycine trifluoroethyl ester), fPhe-glycol (Supporting Information, Figure 9), fPhe-OMe (Supporting Information, Figure 10), fAla-OMe (Supporting Information, Figure 10), and fGly-OMe (Table 2).

DISCUSSION

The reaction of fPhe-TFE with glycinamide addresses several potential shortcomings of a previous model reaction between fGly-glycol and Tris. In addition to the first-order reaction of glycinamide with fPhe-TFE, whose rate constant was the objective of the present experiments, the rate expression contained a second term consistent with general base catalysis by a second molecule of amine (*15*, *27*, *28*). The absence of that term in the earlier reaction with Tris seemed anomalous, suggesting that the mechanism of the Tris reaction might be atypical, possibly involving initial attack by oxygen (see introductory remarks). An additional advantage of the present model reaction is that the basicity of the conjugate base of trifluoroethanol ($pK_a = 12.4$, see Table 1) more closely approximates the basicity of the leaving 3′-OH group of the terminal adenosine of tRNA ($pK_a = 12.98$, *19*) than do those of ethylene glycol ($pK_a = 14.8$, *20*) or methanol ($pK_a = 15.5$, *20*), which were used in the previous study. [It may also be worth noting that the derivatives of glycine used in the earlier model studies are usually somewhat more reactive than those of other amino acids, as exemplified by the entries for fGly-OMe and fPhe-OMe in Table 2 (see also Greenstein and Winitz, *29*)].

Rate constants and thermodynamic parameters for the present uncatalyzed (or water-catalyzed; *vide infra*) model reaction, for the ribosomal reaction, and for the previous model reaction are summarized in Table 3. The rate enhancement produced by the ribosome (3×10^7) is calculated by dividing the second-order ribosomal rate constant (k_{cat}/K_M) by the second-order rate constant for the uncatalyzed reaction (k_1). Earlier, k_{cat}/K_M was shown to be limited by the rate of a chemical process in the ribosome reaction rather than by a binding event (*14*).

Most single-substrate (or hydrolytic) enzymes enhance reaction rates by lowering heats of activation. That behavior is consistent with the formation of new hydrogen bonds and electrostatic interactions in the transition state, as for example in general acid/base catalysis. Because there is no second substrate, or the second substrate (water) is present in abundance, the usefulness of proximity effects is reduced or nonexistent in one-substrate reactions. Thus, it seems understandable that entropic effects are minor in catalysis by those enzymes, with a change in the entropy of activation that approaches zero (*1*, see Figure 6).

In the ribosome, the rate enhancement is entirely entropic in origin. In fact, the enthalpic barrier to the bisubstrate reaction within the ribosome is actually *higher* than the reaction in solution by nearly 8 kcal/mol. And while the solution reaction is entropically unfavorable ($T\Delta S^{\ddagger}$ is large and negative), the *increase* in $T\Delta S^{\ddagger}$ approaches 18 kcal/mol (Figure 6), more than sufficient to account for the rate enhancement produced by the ribosome. That rate enhancement (3×10^7) is relatively modest compared with a typical value of 10^{12} to 10^{14} for single-substrate or hydrolytic enzymes (*30*), as might be expected for a mechanism dependent entirely on physical effects.

The entropic effect of the ribosome may include contributions from two potential sources of catalysis that cannot be distinguished on the basis of present experimental evidence. First, the ribosome might juxtapose the substrates in a position conducive to reaction, reducing the translational and rotational entropy costs associated with complex formation in solution. Interestingly, the observed rate enhancement for this reaction approaches the maximum value expected of a purely "entropic" catalyst (10^8, *2*). A second possibility arises from the presumably zwitterionic nature of the transition state for ester aminolysis. The solvent retardation observed in the present model for peptidyl transfer is consistent with the likelihood that two neutral species combine to form a more polar transition state. Formation of this zwitterionic transition state within the essentially desolvated peptidyl-transferase center of the ribosome would avoid the entropic cost of organizing solvent water around this species in free solution, accelerating the reaction. This latter alternative is supported by theoretical calculations and molecular dynamics simulations conducted by Warshel (*31*) and Åqvist (*32*, *33*) and their associates. It seems likely that the action of the ribosome depends on some combination of juxtaposition and desolvation effects.

Weinger et al. have established that a vicinal 2′-OH group must be present in peptidyl-tRNA for peptidyl transfer to occur rapidly within the ribosome (*34*). Thus, the rate of peptidyl transfer is reduced by a factor of 10^6 when the 2′-OH group is removed. They have described that effect, appropriately, as "*substrate assistance*". Effects of this kind have also sometimes been described as "*substrate-assisted catalysis*", a term that may be less fortunate because of its potential for confusion. As noted above, the zwitterionic transition state for peptidyl transfer is expected to be more strongly solvated by water than are the substrates in the ground state. In view of the existence of an additional reaction pathway for ester aminolysis that involves general base catalysis by amine, it seems reasonable to suppose that solvent water also acts as a general base catalyst for this reaction. Water has been implicated in a similar role for the related hydrolysis of esters and anhydrides because it falls on the same linear Brønsted plot as do other general bases for that reaction (for a more complete treatment of this subject, see ref *35* and references cited therein). The water reactions of those compounds are also associated with extraordinarily large and negative entropies of activation

Table 3: The Thermodynamic Activation Parameters[a,b] for Model and Ribosomal Reactions

	amine	ester	rate constant[c]	$\Delta G^{\ddagger}$	$\Delta H^{\ddagger}$	$T\Delta S^{\ddagger}$
uncatalyzed[d]	**glycinamide**	**fPhe-TFE**	$\mathbf{3 \times 10^{-5}}$	**23.5** ± 0.7	**7.8** ± 0.4	**−15.7** ± 0.8
ribosome (*E. coli*)[e]	**puromycin**	**fMet-tRNA^{fMet}**	$\mathbf{1 \times 10^{3}}$	**14.0**	**16.0**	**2.0**
uncatalyzed[e]	Tris	fGlyglycol	3×10^{-4}	22.2	9.1	−13.0
uncatalyzed[f]	Tris	fMet-tRNA^{fMet}	1×10^{-4}	22.7	16.2	−6.5

[a] Comparisons that seem most appropriate are shown in boldface. Reactions with Tris appear to involve complications (see text). [b] Values reported in units of kcal/mol. [c] Values reported in units of M^{-1} s^{-1}. [d] This work. [e] References *13*, *14*. [f] Reference *12*.

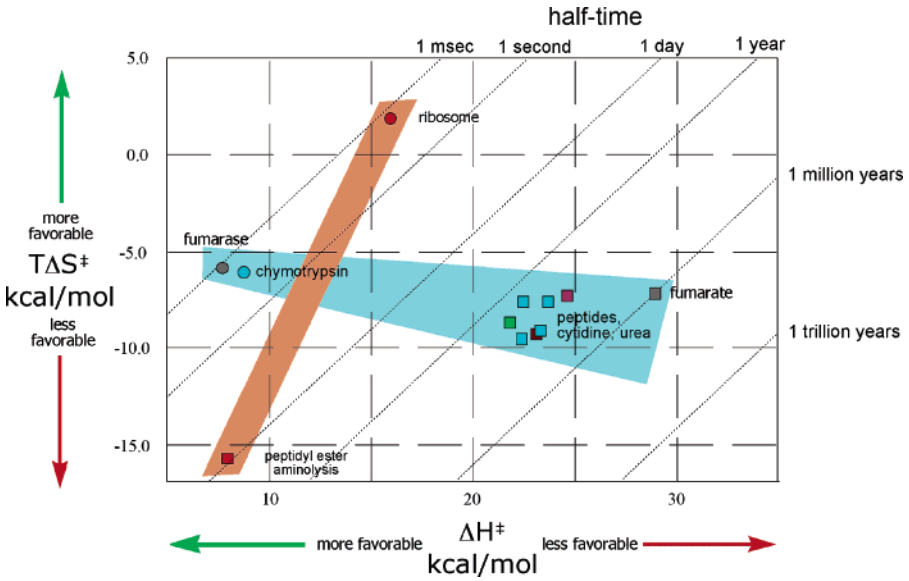

FIGURE 6: Heats and entropies of activation for model uncatalyzed reactions representative of peptide hydrolysis (blue, green, maroon, pink, or gray filled squares) and peptide synthesis (red filled square, this work) compared with k_{cat} for the corresponding hydrolytic enzyme (blue or gray filled circles) or k_{cat}/K_m for the ribosome-catalyzed reaction (red filled circle), respectively. The blue shaded portion of the diagram indicates that the rate enhancements of hydrolytic reactions are predominantly based on lowering heats of activation, while the orange shaded region indicates that the ribosome catalyzes peptide synthesis by rendering the entropy of activation more favorable.

(*36*, *37*). But ordinarily, when one speaks of the effect of substrate structure on the catalytic proficiency of an enzyme, one refers to interactions between a substrate and catalyst that enhance the rate of the catalyzed reaction above the rate of reaction in water in the absence of a catalyst. Judged by that criterion, the 2′-OH group of peptidyl-tRNA may not be formally catalytic, although it becomes essential for reaction within the special context of the ribosome. As has been recognized by other authors (*38*, *39*), the principal role of the 2′-OH group may simply be to assume the role that water molecules play in ester aminolysis in aqueous solution. As shown earlier (*14*, *40*, *41*), and in the present work (Table 2, comparing the uncatalyzed reaction rate of fPhe-glycol with that of fPhe-OMe), a vicinal −OH group exerts only a minor effect on the reactivity of esters with amine or hydroxide ion nucleophiles when water is present in abundance.

It remains possible, of course, that the 2′-OH group of peptidyl-tRNA also causes some structural reorganization within the ribosome. But it remains to be demonstrated that the 2′-OH group makes any additional contribution to the overall rate enhancement that extends beyond mere compensation for the absence of solvent water as a catalyst.

CONCLUDING REMARKS

In summary, the present aminolysis reaction differs from earlier model reactions (*14*) in that it (A) incorporates a leaving group whose pK_a value approaches that of tRNA, (B) exhibits general base catalysis by amine (as well as "uncatalyzed" aminolysis), and (C) employs a simple amine that does not participate in undesirable side reactions. For these reasons, this reaction appears to furnish a more robust model for the ribosomal reaction. The paradoxical absence of any apparent effect of a neighboring −OH group on the rate of ester aminolysis in water (which stands in contrast to the presence of a marked −OH group effect on the rate of reaction in the ribosome) can be understood in terms of the likelihood that, in the ribosome, this −OH group replaces solvent water as a catalyst. Interestingly, Petkov et al. have shown that the vicinal 2′-OH group increases the rate of peptidyl adenosine ethanolysis by ~600-fold in the absence of water (*42*). Together with the results of other biochemical investigations (*8*−*12*), the present results leave no compelling reason to suppose that the ribosome itself acts as a chemical catalyst in any conventional sense. Instead, the ribosome appears to act entirely by a combination of propinquity and desolvation effects.

ACKNOWLEDGMENT

The authors thank Gregory Young for his kind assistance with NMR data acquisition and Charles Lewis for discussions and help in the preparation of this manuscript.

SUPPORTING INFORMATION AVAILABLE

Additional spectra pertaining to the synthesis of fPhe-TFE and its subsequent reaction with glycinamide (along with

the corresponding solvent and salt effects), information on the pK_a determination of *N*-formylphenylalanine, a plot of the temperature dependence of the pD of a glycinamide solution, and representative plots for the aminolysis of both ethylene glycol and methyl esters. This material is available free of charge via the Internet at http://pubs.acs.org.

REFERENCES

1. Wolfenden, R., Snider, M., Ridgway, C., and Miller, B. (1999) The temperature dependence of enzyme rate enhancements, *J. Am. Chem. Soc. 121*, 7419−7420.
2. Page, M. I., and Jencks, W. P. (1971) Entropic contributions to rate accelerations in enzymic and intramolecular reactions and the chelate effect, *Proc. Natl. Acad. Sci. U.S.A. 68*, 1678−1683.
3. Wolfenden, R. (1972) Analog approaches to the structure of the transition state in enzyme reactions, *Acc. Chem. Res. 5*, 10−18.
4. Crick, F. H. (1958) On protein synthesis, *Symp. Soc. Exp. Biol. 12*, 138−163.
5. Welch, M., Chastang, J., and Yarus, M. (1995) An inhibitor of ribosomal peptidyl transferase using the transition-state analogy, *Biochemistry 34*, 385−390.
6. Ban, N., Nissen, P., Hansen, J., Moore, P. B., and Steitz, T. A. (2000) The complete atomic structure of the large ribosomal subunit at 2.4 Å resolution, *Science 289*, 905−920.
7. Huang, K. S., Weinger, J. S., Butler, E. B., and Strobel, S. A. (2006) Regiospecificity of the peptidyl tRNA ester within the ribosomal P site, *J. Am. Chem. Soc. 128*, 3108−3109.
8. Rodnina, M. V., Beringer, M., and Wintermeyer, W. (2007) How ribosomes make peptide bonds, *Trends Biochem. Sci. 32*, 20−26.
9. Sato, N. S., Hirabayashi, N., Agmon, I., Yonath, A., and Suzuki, T. (2006) Comprehensive genetic selection revealed essential bases in the peptidyl-transferase center, *Proc. Natl. Acad. Sci. U.S.A. 103*, 15386−15391.
10. Rodnina, M. V., Beringer, M., and Wintermeyer, W. (2006) Mechanism of peptide bond formation on the ribosome, *Q. Rev. Biophys. 39*, 203−225.
11. Bieling, P., Beringer, M., Adio, S., and Rodnina, M. V. (2006) Peptide bond formation does not involve acid-base catalysis by ribosomal residues, *Nat. Struct. Mol. Biol. 13*, 423−428.
12. Beringer, M., Bruell, C., Xiong, L., Pfister, P., Bieling, P., Katunin, V. I., Mankin, A. S., Böttger, E. C., and Rodnina, M. V. (2005) Essential mechanisms in the catalysis of peptide bond formation on the ribosome, *J. Biol. Chem. 280*, 36065−36072.
13. Sievers, A., Beringer, M., Rodnina, M. V., and Wolfenden, R. (2004) The ribosome as an entropy trap [Erratum], *Proc. Natl. Acad. Sci. U.S.A. 101*, 12397−12398.
14. Sievers, A., Beringer, M., Rodnina, M. V., and Wolfenden, R. (2004) The ribosome as an entropy trap, *Proc. Natl. Acad. Sci. U.S.A. 101*, 7897−7901.
15. Jencks, W. P., and Gilchrist, M. (1966) General base catalysis of the aminolysis of phenyl acetate by primary alkylamines, *J. Am. Chem. Soc. 88*, 104−108.
16. De Jersey, J., Fihelly, A. K., and Zerner, B. (1980) On the mechanism of the reaction of tris(hydroxymethyl)aminomethane with activated carbonyl compounds: a model for the serine proteinases, *Bioorg. Chem. 9*, 153−162.
17. Jencks, W. P., and Carriuolo, J. (1960) Reactivity of nucleophilic reagents toward esters, *J. Am. Chem. Soc. 82*, 1778−1786.
18. Bruice, T. C., and York, J. L. (1961) Mechanism of the reaction of tris(hydroxymethyl)aminomethane and pentaerythritol with phenyl esters, *J. Am. Chem. Soc. 83*, 1382−1387.
19. Åström, H., Limén, E., and Strömberg, R. (2004) Acidity of secondary hydroxyls in ATP and adenosine analogues and the question of a 2′,3′-hydrogen bond in ribonucleosides, *J. Am. Chem. Soc. 126*, 14710−14711.
20. Jencks, W. P. (1968) in *Handbook of Biochemistry* (Sober, H. A., Ed.) pp J150−J189, Chemical Rubber Co., Cleveland, OH.
21. Fersht, A. R., and Requena, Y. (1971) Mechanism of the α-chymotrypsin-catalyzed hydrolysis of amides. pH dependence of k_c and K_m. Kinetic detection of an intermediate, *J. Am. Chem. Soc. 93*, 7079−7087.
22. Good, N. E., Winget, G. D., Winter, W., Connolly, T. N., Izawa, S., and Singh, R. M. M. (1966) Hydrogen ion buffers for biological research, *Biochemistry 5*, 467−477.
23. Donghi, D., Beringhelli, T., D'Alfonso, G., and Mondini, M. (2006) NMR investigation of the dihydrogen-bonding and proton-transfer equilibria between the hydrido carbonyl anion $[HRe_2(CO)_9]^-$ and fluorinated alcohols, *Chem.—Eur. J. 12*, 1016−1025.
24. Zief, M., and Edsall, J. T. (1937) Studies in the physical chemistry of amino acids, peptides and related substances. IX. The dissociation constants of some amino acid derivatives, *J. Am. Chem. Soc. 59*, 2245−2248.
25. Salomaa, P., Schaleger, L. L., and Long, F. A. (1964) Solvent deuterium (D) isotope effects on acid-base equilibriums, *J. Am. Chem. Soc. 86*, 1−7.
26. Goldberg, R. N., and Hepler, L. G. (1968) Thermodynamics of ionization of deuterium oxide, *J. Phys. Chem. 72*, 4654−4659.
27. Bruice, T. C., and Benkovic, S. J. (1964) The compensation in $\Delta H^{\ddagger}$ and $\Delta S^{\ddagger}$ accompanying the conversion of lower order nucleophilic displacement reactions to higher order catalytic processes. The temperature dependence of the hydrazinolysis and imidazole-catalyzed hydrolysis of substituted phenyl acetates, *J. Am. Chem. Soc. 86*, 418−426.
28. Bruice, T. C., and Mayahi, M. F. (1960) The influence of the leaving tendency of the phenoxy group on the ammonolysis and hydrolysis of substituted phenyl acetates, *J. Am. Chem. Soc. 82*, 3067−3071.
29. Greenstein, J. P., and Winitz, M. (1961) *Chemistry of the Amino Acids*, p 926, Wiley, New York.
30. Wolfenden, R. (2006) Degrees of difficulty of water-consuming reactions in the absence of enzymes, *Chem. Rev. 106*, 3379−3396.
31. Sharma, P. K., Xiang, Y., Kato, M., and Warshel, A. (2005) What are the roles of substrate-assisted catalysis and proximity effects in peptide bond formation by the ribosome?, *Biochemistry 44*, 11307−11314.
32. Trobro, S., and Åqvist, J. (2006) Analysis of predictions for the catalytic mechanism of ribosomal peptidyl transfer, *Biochemistry 45*, 7049−7056.
33. Trobro, S., and Åqvist, J. (2005) Mechanism of peptide bond synthesis on the ribosome, *Proc. Natl. Acad. Sci. U.S.A. 102*, 12395−12400.
34. Weinger, J. S., Parnell, K. M., Dorner, S., Green, R., and Strobel, S. A. (2004) Substrate-assisted catalysis of peptide bond formation by the ribosome, *Nat. Struct. Mol. Biol. 11*, 1101−1106.
35. Jencks, W. P. (1969) *Catalysis in Chemistry and Enzymology*, pp 170−173 and 513, McGraw-Hill, New York.
36. Di Sabato, G., Jencks, W. P., and Whalley, E. (1962) Effect of pressure on the spontaneous hydrolysis of acetyl phosphate monoanion and dianion and of acetyl phenyl phosphate monoanion, *Can. J. Chem. 40*, 1220−1224.
37. Koskikallio, J., Pouli, D., and Whalley, E. (1959) Pressure effect and mechanism in acid catalysis. V. Hydrolysis of acetic anhydride, *Can. J. Chem. 37*, 1360−1366.
38. Weinger, J. S., and Strobel, S. A. (2006) Participation of the tRNA A76 hydroxyl groups throughout translation, *Biochemistry 45*, 5939−5948.
39. Rangelov, M. A., Vayssilov, G. N., Yomtova, V. M., and Petkov, D. D. (2006) The syn-oriented 2-OH provides a favorable proton transfer geometry in 1,2-diol monoester aminolysis: implications for the ribosome mechanism, *J. Am. Chem. Soc. 128*, 4964−4965.
40. Wolfenden, R. (1963) The mechanism of hydrolysis of amino acyl RNA (ribonucleic acid), *Biochemistry 2*, 1090−1092.
41. Bruice, T. C., and Fife, T. H. (1962) Hydroxyl group catalysis. III. The nature of neighboring hydroxyl group assistance in the alkaline hydrolysis of the ester bond, *J. Am. Chem. Soc. 84*, 1973−1979.
42. Changalov, M. M., Ivanova, G. D., Rangelov, M. A., Acharya, P., Acharya, S., Minakawa, N., Földesi, A., Stoineva, I. B., Yomtova, V. M., Roussev, C. D., Matsuda, A., Chattopadhyaya, J., and Petkov, D. D. (2005) 2′/3′-O-peptidyl adenosine as a general base catalyst of its own external peptidyl transfer: implications for the ribosome catalytic mechanism, *ChemBioChem 6*, 992−996.

BI602600P